

# Modelling of Creep in Nickel Based Superalloys

A. P. Miodownik<sup>1</sup>, X.Li<sup>2</sup>, N. Saunders<sup>1</sup>, and J.-Ph. Schille<sup>2</sup>

Thermotech Ltd<sup>1</sup> and Sente Software Ltd<sup>2</sup>

Surrey Technology Centre, The Surrey Research Park, Guildford GU2 7YG, U.K.

## Abstract

A new software programme, JMatPro, is used to obtain steady state creep rates and creep rupture life for multi-component commercial nickel based alloys. A key feature of the programme is that overall properties are obtained through calculation and combination of the properties of individual phases. This includes thermodynamic properties, thermo-physical and physical properties, mechanical properties, and derivative properties such as anti-phase boundary and stacking fault energies. Access to such properties allows the self-consistent calculation of the required input parameters for a standard dislocation creep equation. This is in contrast to many previous attempts that have had to use empirical values for various critical parameters, such as stacking fault energies, anti-phase boundary energies and various elastic moduli, which are all dependent on temperature as well as composition. It is shown that calculations can be made for any desired alloy by entering only the composition of the alloy, the size(s) of  $\gamma'$  and/or  $\gamma''$  (if present), the creep temperature and the applied stress. Good agreement has been obtained between the calculated secondary creep rates/rupture life and the observed results for many commercial nickel based superalloys.

## Introduction

Understanding the factors affecting the performance of Ni-based superalloys is vital to the industrial gas turbine industry and many formulations have been proposed to calculate the secondary creep rates.<sup>1,2,3,4,5</sup> While engineering requirements require the properties of the alloy as a whole to be described, it is the properties of individual phases and microstructural features that play the fundamental role in determining overall properties and which are a necessary input into physically based models. However, values for critical input parameters referring to individual phases are often missing, especially for complex multi-component industrial alloys. In the absence of data related to specific alloys and temperatures, previous treatments have often had to use empirically determined values for important parameters such as the modulus, stacking fault energy or APB energies. This makes it difficult to judge whether a particular approach would still be applicable outside the limited range of alloy composition or temperatures used to justify the initial equations. More importantly, the effect of changing composition and other variables within or outside specification cannot be estimated properly when input parameters are assumed independent of these variables.

The present paper has several objectives. Firstly to show that it is now possible to systematically calculate secondary creep rates and stress rupture life, not only for the wide range of superalloys currently available, but also for new combination of elements that are being

suggested for the design of the next generation of alloys. It will be shown that most of the required parameters can be calculated, thus leaving far fewer factors to be empirically determined by comparing theory and experiment. The present approach does not remove the necessity of making experiments, but it does substantially reduce the degree of empiricism inherent in many previous treatments. This can markedly reduce the number of trial experiments when developing new alloys, testing the effect of variations within specification limits, and determining the permissible range of heat-treatments.

## Calculation Method

The present work uses a common formulation (eq.1) for the secondary creep rate<sup>2</sup> that features both a back stress function and takes the stacking fault energy ( $\gamma_{SFE}$ ) explicitly into account<sup>6</sup>. This approach was selected as it contains parameters that have an identifiable physical basis and which can be calculated self-consistently.

$$\dot{\epsilon} = AD_{eff} \left[ \frac{\gamma_{SFE}}{Gb} \right]^n \left[ \frac{\sigma - \sigma_0}{E} \right]^m \quad (1)$$

where  $\dot{\epsilon}$  is the secondary creep rate, A is a structure-dependent parameter,  $D_{eff}$  is the effective diffusion coefficient,  $\gamma$  is the stacking fault energy of the matrix, b is the burgers vector,  $\sigma$  is the applied stress,  $\sigma_0$  is the back stress, with G and E the shear and Young's modulus of the matrix phase at the creep temperature respectively. The back stress  $\sigma_0$ , is calculated following the treatment of Lagneborg and Bergman<sup>5</sup>, setting  $\sigma_0 = 0.75\sigma$  when  $\sigma < \frac{4}{3}\sigma_p$ , (where  $\sigma_p$  is the critical back stress from strengthening due to precipitates) and  $\sigma_0 = \sigma_p$  when  $\sigma > \frac{4}{3}\sigma_p$ . The exponents n and m exhibit a range of values in the literature, but in this paper have been given fixed values of n=3 and m=4.

A basic feature of JMatPro is that the overall properties of complex materials are calculated by combining the properties of individual phases. It is therefore necessary to start by calculating reliable volume fractions of all the constituent phases over the temperature range of interest. This is achieved for multi-component alloys by combining a suitable thermodynamic database<sup>7,8</sup> with a fast minimisation engine,<sup>9</sup> following the well-established CALPHAD technique.<sup>10</sup> For the calculation of secondary creep rates in the alloys concerned here, the key phases are  $\gamma$ ,  $\gamma'$  and  $\gamma''$ .

The next step is to consider the properties of individual phases, such as the  $\gamma_{SFE}$  for the matrix phase, which is directly required by eq.1. Experimental values of  $\gamma_{SFE}$  are usually only available for rather simple alloys and over a limited temperature range, often just room temperature.

JMatPro calculates as many parameters as possible from more basic data held in the programme, in order to minimise the creation of separate databases. While the latter are required for moduli and diffusion calculations, it will be seen that this can be avoided in most other cases. For example, the  $\gamma_{SFE}$  at the creep temperature is calculated from the Gibbs free energy difference between *fcc* and *hcp* structures,<sup>11</sup> which is readily available by using a CALPHAD calculation.

A second example is given by the calculation of the critical back stress  $\sigma_p$ , which is directly related to the strengthening contribution of the  $\gamma'$  and  $\gamma''$  phases, through a proportionality constant and the volume fractions of  $\gamma'$  and  $\gamma''$ . For the case of  $\gamma'$ , this can be calculated using the approach detailed in Saunders et al..<sup>9</sup> For the case of  $\gamma''$  a slightly different approach is used – in

this case a contribution for strain hardening is included due to the large lattice misfit in the major axis of the  $\gamma'$  precipitates.<sup>12</sup> Fig.1 shows a comparison of calculated and measured<sup>3,5,13,14,15</sup> values for  $\sigma_p$ . The agreement is quite good. Further work is being undertaken to develop a more general approach that is applicable to other strengthening phases.

The various moduli have been calculated using databases for  $E$  and Poisson's ratio ( $\nu$ ), such that only the composition of the matrix and temperature are required to obtain  $G$  and  $E$ <sup>16</sup>. The diffusion coefficient  $D_{\text{eff}}$  in the above equation is concentration dependent and calculated using the following expressions.<sup>17</sup>

$$D_{\text{eff}} = D_o \exp(-Q_{\text{eff}} / RT) \quad (2a)$$

where

$$D_o = \sum_i x_i D_i^0 \quad (2b)$$

and

$$Q_{\text{eff}} = \sum_i x_i Q_i \quad (2c)$$

In equations 2b and 2c,  $x_i$  is the mole fraction of element  $i$  in the matrix and  $D_i^0$  and  $Q_i$  are, respectively, the frequency factor and activation energy for diffusion of element  $i$  in the matrix. Although cross terms are neglected, this approach has been previously validated during application to other kinetic phenomena such as TTT curves<sup>9,17</sup> and particle coarsening.<sup>18</sup>

Reference to eq.1 shows that the only remaining floating parameter is  $A$ . If the above treatment is valid, only a single value of  $A$  should be required to make viable predictions for secondary creep rates, with the proviso that all the alloys concerned have similar microstructural features. The latter requirement signals that difficulties may arise in achieving a single treatment for both solid solution alloys and alloys containing precipitates. In practice we have found that  $A$  is a function of the volume fraction ( $V_f$ ) of  $\gamma'$  and  $\gamma''$  and the following equation has been used:

$$A = \frac{10.0^{19.7}}{V_f + 0.005} \quad (3)$$

The need for such an expression arises from the much faster creep rates for solid solution alloys, in comparison to  $\gamma'$  or  $\gamma''$  hardened alloys. However even after using eq.3, the general scatter for solid solution alloys is greater, which suggests that additional variations in the underlying hardening mechanisms need to be addressed.<sup>19</sup>

## Results

Figure 2 shows the correlation for a very wide range of polycrystalline alloys calculated using the approach described above. The experimental data for creep rates has been drawn from a wide range of references.<sup>2,3,5,13,14,20,21,22,23,24,25</sup> Where possible, we have calculated  $\sigma_p$  using information of  $\gamma'$  and  $\gamma''$  particle sizes reported by the authors, or have used values which can be reasonably estimated from analogous alloys. A specific comparison for the stress dependence of

secondary creep rates in Nimonic 80A is given in Fig.3. Curves can be generated to examine the effect of all the other variables in eq.1 together with changes in composition and temperature.

The behaviour of single crystal alloys has also been examined, but has not been included in the present paper as this requires a more complicated treatment involving orientation factors and also a slightly different value of  $A$ .

### ***Extension to the calculation of rupture strength***

As rupture strength is an alternative design criterion in many practical cases, the calculation procedure has been extended to include this property by using the relationship suggested by Davies and Wilshire.<sup>26</sup>

$$t_r = a\dot{\epsilon}^b \quad (4)$$

where  $t_r$  is the time to rupture,  $a$  and  $b$  are constants and  $\dot{\epsilon}$  is the secondary creep rate. The correlation between the experimental secondary creep rates and creep rupture life for various Ni-based superalloys is given in Fig.4. The experimental data has been drawn from the following references.<sup>23,27,28,29,30,31</sup>

This useful relationship will, however, only hold if the structure of the alloy remains reasonably stable with time during creep. If the situation refers to short times and relatively low temperatures, then it should still be possible to compare calculation with experiment, even if applied stresses are high, as the microstructure will remain relatively stable.

This has been checked for  $\gamma'$  or  $\gamma''$  hardened disk alloys against the 1000hr rupture strength reported by Sims et al.<sup>32</sup> For the most part comparison is made with the rupture strength given at 760°C by Sims et al.<sup>32</sup> because many disk alloys have a final heat treatment close to 750°C. In this case the amount of  $\gamma'$  and  $\gamma''$  formed after heat treatment will remain stable and coarsening rates sufficiently low to prevent substantial degradation in creep rupture life. Fig.5 shows a comparison of calculated and experimental stress rupture behaviour for a variety of disk alloys.

For two cases, the final heat treatment is at 850°C and we have made the calculation at 870°C for comparison with experimental rupture strength reported at this temperature. For four alloys the final heat treatment temperature is closer to 650°C and we have therefore used the 650°C rupture stress for comparison. For the case of Udimet 720 only the 650°C rupture strength is given. In this case the amount of  $\gamma'$  at 650° and 750°C is very similar and we have used the strength calculated at 750°C in calculating 650°C rupture strength. For the present, we have not included alloys which exhibit carbide hardening or solid solution hardened alloys, where we have noted that calculated results invariably underestimate rupture strengths. Further work will be undertaken to address this issue.

Where the results presented in standard source books give no information on particle size, we have estimated  $\sigma_p$  in the following way. First, the strength of the solid solution matrix is calculated based on the composition of the matrix at the heat treatment temperature, using a standard grain size of 100  $\mu\text{m}$ . As Sims et al.<sup>32</sup> also report the final 0.2% proof stress after heat treatment, the strengthening contribution of the  $\gamma'$  and  $\gamma''$  particles can therefore be readily extracted.

## Discussion

Considering the relatively simple approach used in the present study, there is really quite remarkable success. It is well understood that the complete modelling of creep is more complex. For example, a more detailed treatment of microstructural stability should be included because, when creep occurs in the stress range where  $\sigma > \frac{4}{3} \sigma_p$  and the temperature is high enough, then the secondary creep rate will vary with time because  $\sigma_p$  will change as  $\gamma'$  and  $\gamma''$  coarsen. In this case, a coarsening module available within JMatPro<sup>9,18</sup> allows an estimate of the resulting degradation of properties and will be integrated within the creep module. Also, a better representation of damage accumulation would lead to a more explicit formulation for the tertiary stage of creep and primary creep must be included if a full creep curve is to be calculated

However, even with its present shortcomings, it is clear that the present approach has some distinct advantages over previous methods. Very few empirical parameters are required, the model has an identifiable physical basis and the calculations are self-consistent. One can therefore expect significant advantages when creep properties need to be extrapolated. Because of the time scales involved, creep experiments are usually performed for periods that are shorter than the real exposure times for industrial gas turbines. Secondly, the approach can be used as part of an alloy design process, where comparative behaviour between various alloys is readily obtained without the need for lengthy experiment.

The model will now be extended so that the shortcomings of the present capability can be overcome and a full creep curve modelled. It is intended to do this by looking at a cumulative function that includes an expression for primary creep as well as a better representation of the effect of tertiary creep. The treatment where there is  $\gamma'$  and/or  $\gamma''$  coarsening, or where there is a phase transformation simultaneously occurring, needs to be improved. For the latter case, TCP phases may remove slow moving elements from the matrix or metastable  $\gamma''$  may transform to the stable  $\delta$  phase. These are further examples where the secondary creep rate will be time dependent and an integration function will need to be applied so that deformation as a function of time is better represented. It should also be possible to include the susceptibility to rafting for single crystals as JMatPro has a capability to accurately calculate  $\gamma/\gamma'$  lattice misfit,<sup>33</sup> as well as make modulus calculations.

## Conclusion

It is possible to calculate steady state creep rates and creep rupture life with the aid of a new software programme, JMatPro. The required input parameters are calculated systematically from the basic properties of individual phases. This substantially reduces the degree of empiricism inherent in many previous treatments and reduces the number of trial experiments when developing new alloys, testing the effect of variations within specification limits and determining the permissible range of heat-treatments. Self-consistent calculations can be made for any desired alloy by entering only the composition, the size of  $\gamma'$  and  $\gamma''$  particles, the creep temperature and the applied stress. Good agreement has been obtained between the calculated secondary creep rates/rupture life and the observed results for many commercial Ni-based superalloys.

## References

1. B. Wilshire and H.E. Evans, *Creep of Metals and Alloys*, Inst. Metals, 1985
2. X.S. Xie, G.L.Chen, P.J. McHugh and J.K. Tien, *Scripta Metall.*, 1982, **16**, 483
3. W.J. Evans and G.F. Harrison, *Metal Science*, 1976, **10**, 307.
4. H. Burt, J. P. Dennison and B. Wilshire, *Metal Science*, 1979, **13**, 295.
5. R. Lagneborg and B. Bergman, *Metal Science*. 1976, **10**, 20.
6. C.R. Barrett and O.D. Sherby, *Trans. Met. Soc. AIME*, (1965), **233**, 1116.
7. N. Saunders, *Superalloys 1996*, R.D. Kissinger et al. eds., TMS, 1996, 101.
8. N. Saunders, M.Fahrman and C.J. Small, *Superalloys 2000*, K.A. Green et al. eds, TMS, 2000, 803
9. N. Saunders, X. Li, A.P. Miodownik and J-Ph. Schillé, *Materials Design Approaches and Experiences*, J.-C. Zhao et al. eds., TMS, 2001, 185.
10. N. Saunders and A. P. Miodownik, *CALPHAD – Calculation of Phase Diagrams*, Pergamon Materials Series vol.1, R.W. Cahn ed., Elsevier Science, 1998.
11. A.P. Miodownik, *CALPHAD*, **2**, 1978, 207.
12. X. Li, N. Saunders, A.P. Miodownik, unpublished research
13. B. Bergman, *Scand. J. Metallurgy*, 1975, **4**, 97.
14. O. Ajaja, T.E. Howson, S. Purushothaman and J.K. Tien, *Mater. Sci. Eng.*, 1980, **44**, 165.
15. Z.A. Yang, Y.I. Xiao and C.H. Shih, *Mat.Sci. Eng.A* 1988, **101**, 65
16. X. Li, A.P. Miodownik and N. Saunders, *J. Phase Equilibria*, 2001, **22**, 247.
17. X. Li, A.P. Miodownik and N. Saunders, *Mater.Sci.Tech.*, 2002, **18**, 861
18. X. Li, N. Saunders and A.P. Miodownik, *Metall.Mater.Trans.A*, 2002, **33A**, 3367
19. Y.Li and T.G. Langdon, *Creep Behaviour of Advanced Materials for the 21st Century*, R.S. Mishra et al. eds., TMS, 1999, 73.
20. W.J. Evans and G.F. Harrison, *Metal Science*, 1979, **13**, 641.
21. R.W. Lund and W.D. Nix, *Acta Met.*, 1976, **24**, 469
22. M.C. Chaturvedi and Y. Han, *Superalloy 718 – Metallurgy and Applications*, E.A. Loria ed. 1989, 489.
23. G. B. Thomas and T. B. Gibbons, *Superalloys 1980*, J.K. Tien et al. eds., TMS, 1980, 699.
24. H.L. Eiselstein and D. J. Tillack, *Superalloys 718, 625 and Various Derivatives*, E.A. Loria ed., TMS, 1991, 1.
25. *Engineering Properties of Alloy 800*, publication 3272A, Henry Wiggin and Co. Ltd.
26. P.W. Davies and B. Wilshire, *Structural Processes in Creep*, A.G. Quarrell ed., Iron and Steel Institute, 1961, 34
27. K. Harris, G. L. Erickson and R. E. Schwer, in *Superalloys 1984*, M. Gell et al. eds., TMS, 1984, 221.
28. F.L. Versnyder and M. E. Shank, *Mater. Sci.Eng.*, 1970, **6**, 213.
29. A. Ferrari, *Superalloys 1976*, Claitor's Publishing Division, 1976, 201
30. D. M. Shah and A. Cetel, *Superalloys 1996*, R.D. Kissinger et al. eds., TMS, 1996, 273.
31. G.E. Korth, *JOM*, January 2000, 40.
32. *Superalloys II*, C.T. Sims et al. eds., Wiley & Sons, 1987
33. N. Saunders, X. Li, A.P. Miodownik and J.-P. Schillé, "The Modelling of Phase Transformations in the Context of a Generalised Materials Property Capability", presented at Int.Symp. Computational Phase Transformations, TMS Annual Meeting, San Diego, March 2-6, 2003

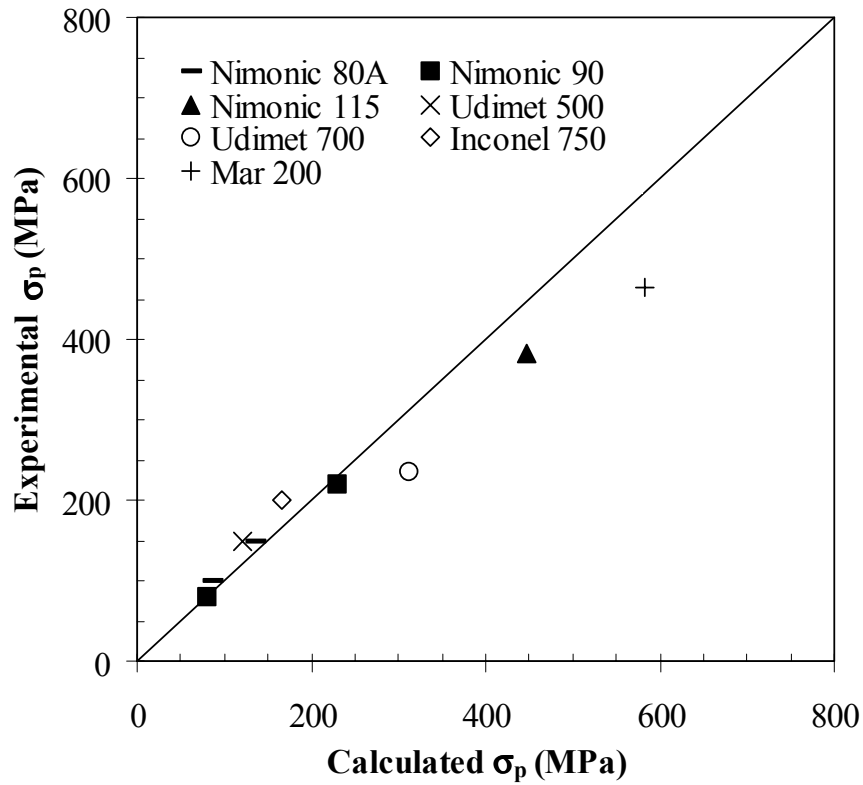


Fig.1 Comparison between calculated and experimental critical back stress. (note for Nimonic 90 and 80A two results are shown, corresponding to different creep temperatures with subsequently different amounts of  $\gamma'$ .)

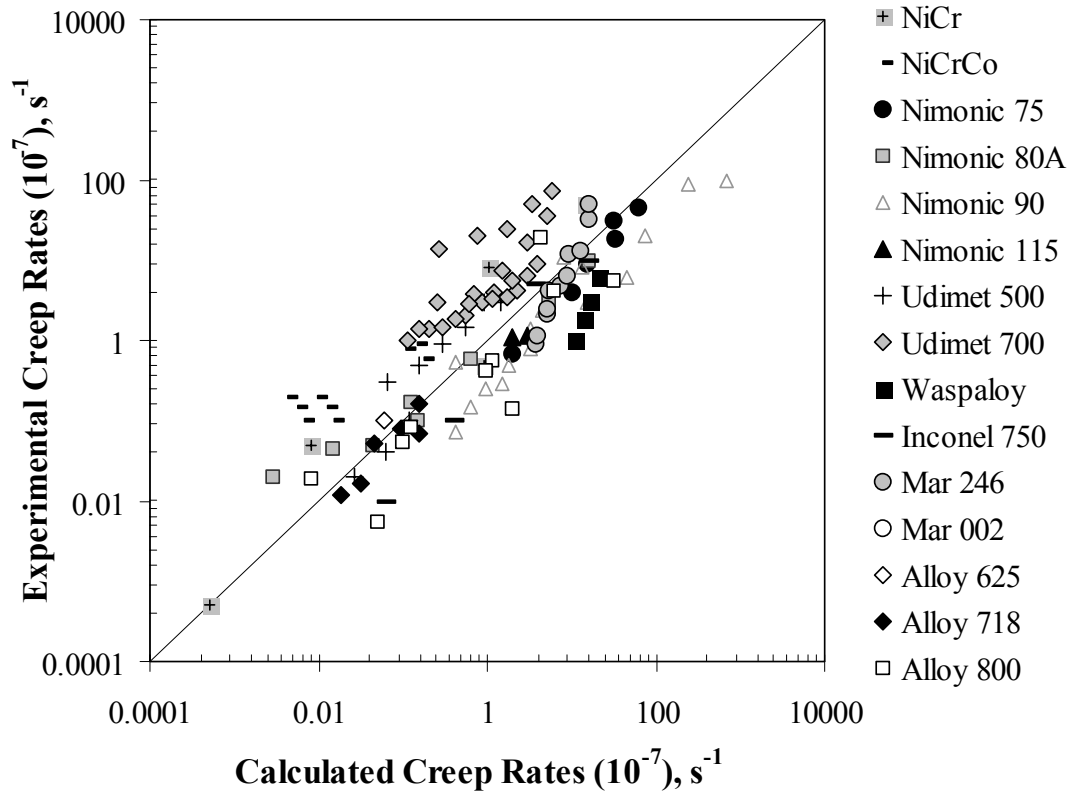


Fig.2 Comparison between calculated and experimentally observed secondary creep rates for a wide range of Ni-based superalloys

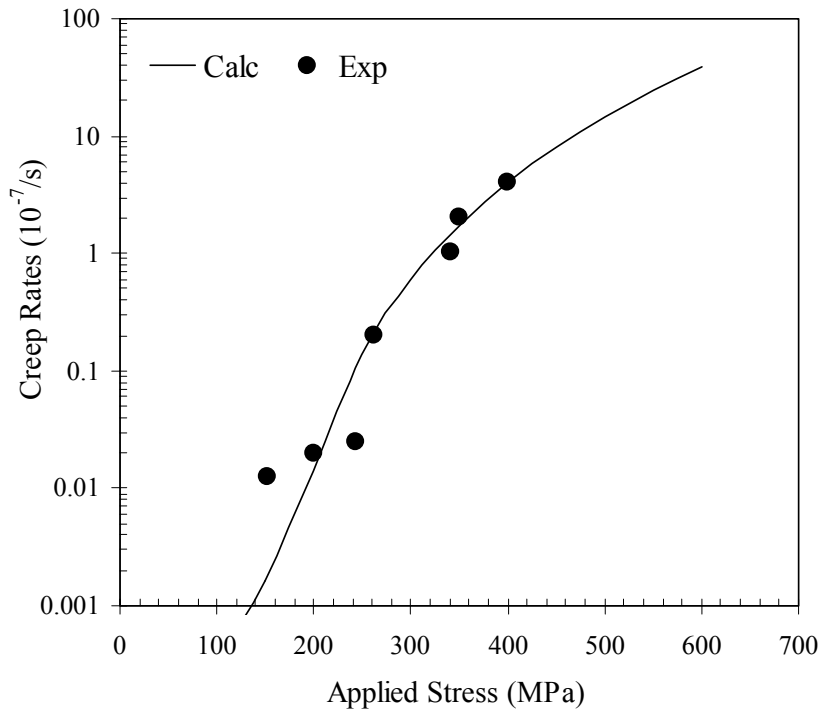


Fig.3 Comparison between calculated and experimentally observed<sup>13</sup> secondary creep rates for Nimonic 80A Ni-based superalloy as a function of applied stress

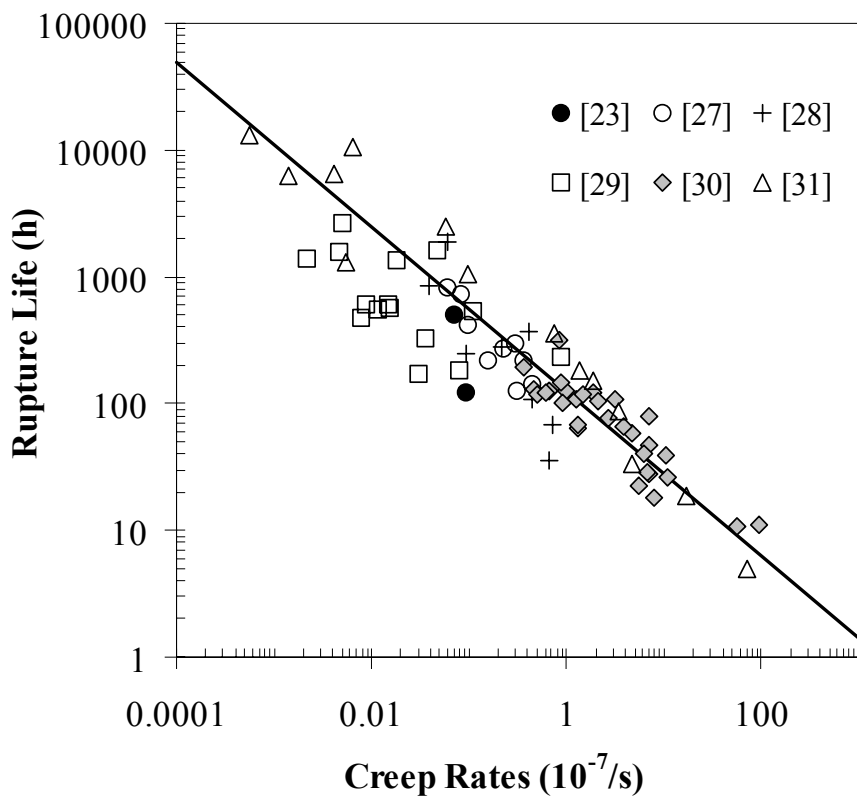


Fig.4 Creep rupture life versus creep rates



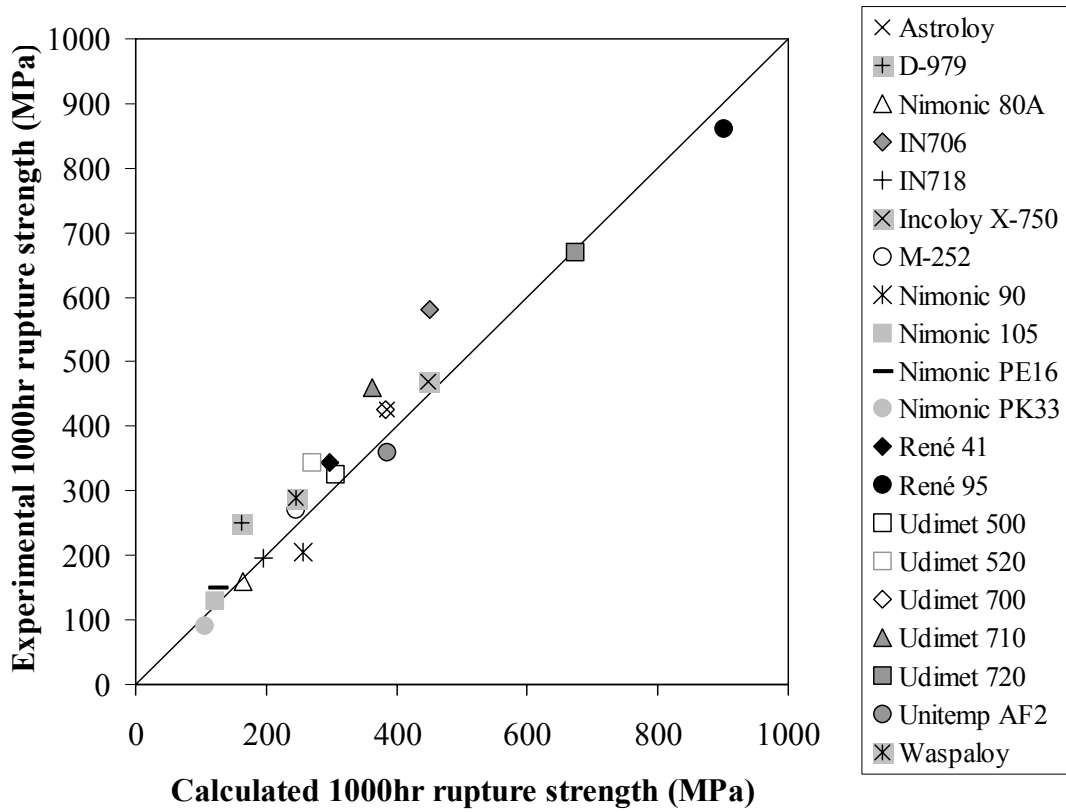


Fig.5 Comparison between experimental<sup>32</sup> and calculated 1000hr Rupture strength for  $\gamma'$  and  $\gamma''$  hardened Ni-based superalloys